

# Reports

## Control of Equatorial Ocean Currents by Turbulent Dissipation

**Abstract.** *The importance of turbulence in the flow of equatorial currents has been noted by modelers but not observed. Recent measurements of turbulence show an increase in strength at the equator and confirm its role as a sink of the kinetic energy of currents at the equator.*

During 1979 and 1980 an intensive meteorological and oceanographic survey of the tropics was conducted under the Global Atmospheric Research Program. To contribute to the program, the Canadian survey ship *Parizeau* spent 2 months in early 1979 as a tropical wind-observing platform at 150°W within a few degrees of the equator. In addition, several oceanographic programs were initiated in the tropical Pacific by American, Canadian, Japanese, Australian, and Peruvian scientists to study variations in the zonal currents, which are thought to cause such diverse phenomena as El Niño in Peru and interannual variations in weather at more northern latitudes (1, 2). The result is the most extensive data set yet of Pacific tropical currents (3). The instrumentation used to make oceanographic observations during the *Parizeau* cruise included velocity microstructure sensors—probes that sense the smallest fluctuations in ocean current velocity. These sensors provided the only direct evidence of turbulence during the Pacific Ocean survey.

In the tropics, the zonal wind blows westward except in the convergence zone between 4° and 10°N, where the winds are weaker and their direction more variable. The westward winds push the surface waters toward the western Pacific. A zonal pressure gradient is created which generates a return flow to the east. One such return flow is the North Equatorial Countercurrent and another is below the surface at the equator, where the Coriolis force diverts all eastward subsurface flow into a jet confined to within ~1° of the equator (2). This Equatorial Undercurrent flows at speeds of 1 to 1.5 m/sec below the wind-driven South Equatorial Current, which flows westward at speeds of up to 1 m/sec. There is large vertical shear at their interface.

The microstructure probes, mounted on a free-falling body called the Camel, give vertical gradients of the two horizontal components of velocity,  $\partial u_1/\partial z$  and  $\partial u_2/\partial z$  (called shears), at scales from 1 to 50 cm and vertical gradients of temperature,  $\partial T/\partial z$ , from 4 cm to larger scales. The two identical shear probes are mounted at right angles for the gradients of the two perpendicular horizontal velocities (4, 5). The scales resolved denote the bounds of the velocity microstructure region at which viscous forces convert turbulent fluctuations to heat. It is the short wavelength end of the turbulence spectrum, and measurements at these wavelengths give the rate of viscous dissipation and an indication of the intensity of turbulence.

Figure 1 summarizes the results of a

single profile through the South Equatorial Current and the Equatorial Undercurrent. Shown are the temperature profile, its depth gradient  $\partial T/\partial z$ , the shear signal  $\partial u/\partial z$  (the filtered output from the shear probe), and the estimated value of viscous dissipation of turbulent energy  $\bar{\epsilon}$ . Measurements with a current meter (6) showed the east-west component of velocity to vary by 130 cm/sec at depths between 24 and 160 m, giving an average large-scale shear of 0.01 sec<sup>-1</sup>, a factor of 100 less than microstructure shears. Turbulence (as indicated by the presence of microstructure shears) is strongest in the upper 140 m, where the large-scale shear is greatest, and decreases in strength below 140 m, where the maximum speed (but minimum large-scale shear) occurs.

The estimate of  $\bar{\epsilon}$  in kinematic units is given by

$$\bar{\epsilon} = \frac{15}{4} \nu \left[ \left( \overline{\frac{\partial u_1}{\partial z}} \right)^2 + \left( \overline{\frac{\partial u_2}{\partial z}} \right)^2 \right]$$

where the overbars denote averaged quantities and  $\nu$  is the kinematic viscosity. The formula assumes isotropy (no directionality), which is expected at microstructure scales. Each horizontal bar in Fig. 1a is the value of  $\bar{\epsilon}$ , over a 2.5-m vertical distance, computed from the variance of the  $\partial u_1/\partial z$  and  $\partial u_2/\partial z$  signals. Although only one of these shears is plotted, both were measured and are statistically similar due to the isotropy of the turbulence at these scales. The left side of each bar is at the noise level of the estimate, produced by

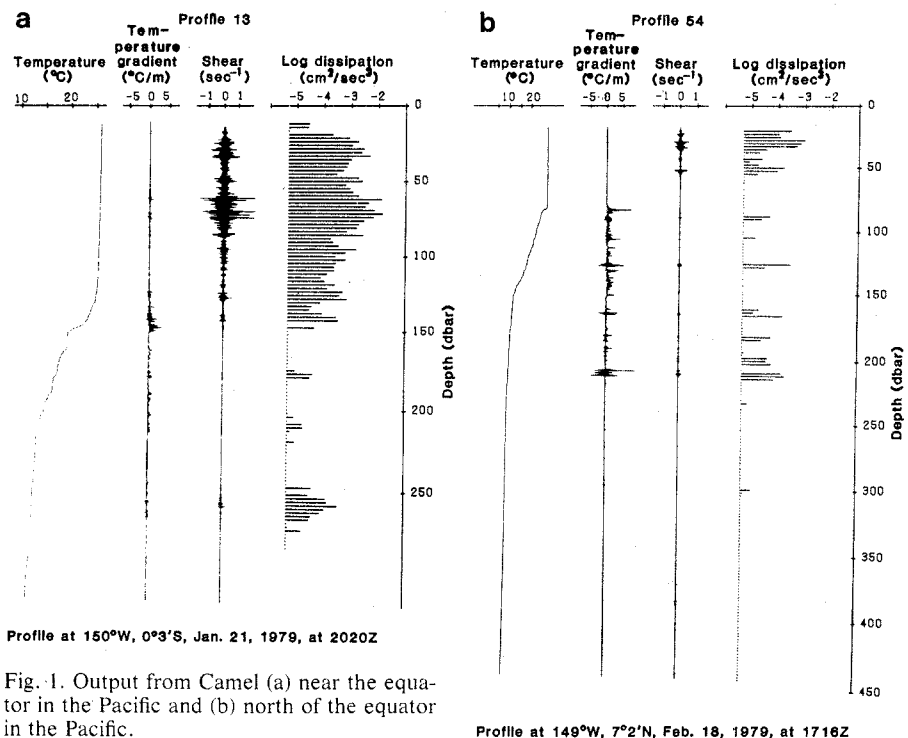


Fig. 1. Output from Camel (a) near the equator in the Pacific and (b) north of the equator in the Pacific.

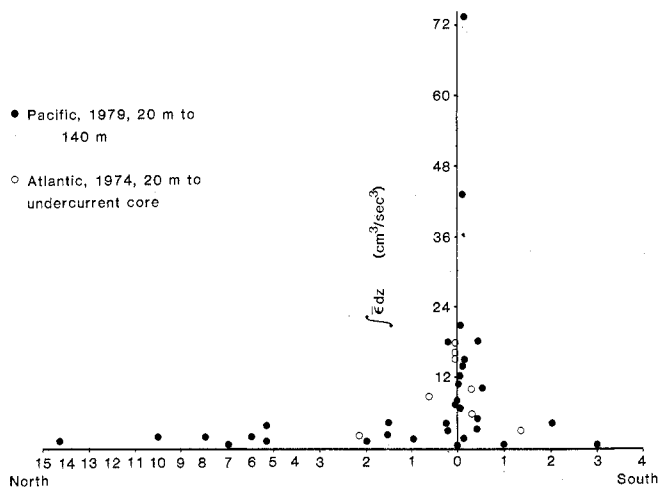


Fig. 2. Integrated dissipation profile. Closed circles represent data gathered during the 1979 cruise of the *Parizeau* in the Pacific. Open circles represent measurements from the research vessel *Atlantis II* in the Atlantic in 1974.

vibrations or thermal contamination, and the right side gives the dissipation estimate on a logarithmic scale. Where only a dot is plotted, the dissipation rate was at or below the noise level. In these regions turbulence was weak or absent.

Very little of this turbulence was found at the depth of the velocity maximum. During the observation period the maximum was found near 150 m, while the depth of maximum dissipation within  $0.5^\circ$  of the equator was at 110 m;  $\bar{\epsilon}$  decreased rapidly below this level (Table 1).

The equatorial regime is confined within  $\sim 1^\circ$  of the equator; a profile from  $7^\circ\text{N}$  is plotted in Fig. 1b to show the change in the nature of turbulence away from the equator. Here the upper wind-mixed layer ends abruptly, with a step change in temperature at 80 m. Turbulent shears are lower than those at the equator. Although no current meter measurements were made at this position, previous measurements have shown no jet in the thermocline similar to the Equatorial Undercurrent. Away from the equator, the wind stress at the surface generates turbulence in the upper layer of the ocean, which entrains water from below and mixes it into the water column. Turbulence above the entrainment depth is stronger than that below it and the interface is sharp. At the equator, mixing between the undercurrent and the westward flowing South Equatorial Current spreads the thermocline, removing the sharp lower boundary. It is the turbulence generated in the zone between the Equatorial Undercurrent and the opposing South Equatorial Current which appears in the profile of  $\partial u/\partial z$  in Fig. 1a.

Although these dissipation estimates do not tell us directly the energy contained in the turbulence or the rate of its production, they reveal more about

these processes than direct measurements could. In stratified fluids turbulence is inefficient at converting its kinetic energy into potential energy through mixing (7). The rate of production is equal to the rate of dissipation to within 20 percent, an error comparable to the confidence limits for the dissipation estimates. These dissipation estimates can thus be interpreted as providing the rate of turbulent energy production (7). The sources of this energy must be the large-scale zonal flow and the wind.

To show the unique nature of the equatorial flow, we plotted the integrated dissipation between 20 and 140 m for each profile taken during the cruise (Fig. 2). The increase in the dissipation rate at the equator is dramatic. For comparison, our 1974 measurements of turbulence in the Atlantic Ocean at  $28^\circ$  and  $33^\circ\text{W}$  are also plotted. The magnitudes are similar, but Pacific Ocean data show less scatter.

Table 1. Dissipations in the Pacific Ocean, averaged over 20-m vertical intervals. The profiles made off the equator were between  $0.5^\circ$  and  $3^\circ\text{S}$  and  $1^\circ$  and  $14^\circ\text{N}$ , in places where the upper mixed layer extended to between 100 and 120 m.

Depth (m)	$\bar{\epsilon}$ [(cm <sup>2</sup> /sec <sup>3</sup> ) 10 <sup>-5</sup> ]	
	Near equator (N = 16)	Off equator (N = 7)
20 to 40	42	24
40 to 60	110	19
60 to 80	160	19
80 to 100	180	13
100 to 120	210	2
120 to 140	33	4
140 to 160	13	5
160 to 180	1	1
180 to 200	0.6	2
200 to 220	0.9	2
220 to 240	0.7	
240 to 260	2	
260 to 280	1	

Just as turbulence at the equator is unique, so are the energetics. The geostrophic balance requires nonequatorial currents to flow nearly parallel to the isobars. The cross-isobar flow, which extracts energy from the pressure field, is relatively small and difficult to measure. At the equator, where the horizontal Coriolis force vanishes, the cross-isobar flow along the zonal pressure gradient produces a large energy flux (8). Data for January and February 1979 are as yet sparse, but historical data (9, 10) obtained at the equator show a per unit mass pressure gradient on the 300 centimeter/ton surface (near 120 m) of  $2 \times 10^{-5}$  cm/sec<sup>2</sup>. A typical value of  $U$  is 100 cm/sec, giving  $U\partial P/\partial x$  equal to  $2 \times 10^{-3}$ , a value close to the equatorial rate of dissipation at that depth (Table 1). The agreement is partly fortuitous, since some energy is radiated away as waves, and seasonal changes alter both the pressure gradient and the current. Nevertheless, these results show that in the absence of the Coriolis force, the flow of the Equatorial Undercurrent is controlled by turbulent friction. A comparison with our measurements in the Atlantic in 1974 shows similar results: the rate of turbulent dissipation in the undercurrent above the core is comparable in magnitude to the rate at which the undercurrent gains energy from the pressure gradient (8).

We can also compute a coefficient of vertical eddy viscosity for the shear region between the South Equatorial Current and the undercurrent by using the near equality of turbulence production and dissipation (4). The eddy viscosity is  $\bar{\epsilon}/(\partial U/\partial Z)^2 = 10$  cm<sup>2</sup>/sec, where  $\bar{\epsilon}$  is averaged between 20 and 140 m and  $\partial U/\partial Z$  is a typical large-scale shear of  $0.01$  sec<sup>-1</sup>.

WILLIAM R. CRAWFORD

*Institute of Ocean Sciences, Sidney, British Columbia, Canada V8L 4B2*

THOMAS R. OSBORN

*Department of Oceanography, University of British Columbia, Vancouver, Canada V6T 1W5*

#### References and Notes

1. *Bull. Am. Meteorol. Soc.* **60**, 244 (1979).
2. K. Wyrtki, *Eos* **60**, 25 (1979).
3. E. Firing, D. Halpern, R. Knox, G. J. McNally, W. C. Patzert, E. D. Stroup, B. A. Taft, R. Williams, *Science* **211**, 22 (1981).
4. W. R. Crawford and T. R. Osborn, *Deep-Sea Res.* **26** (Suppl. 2), 285 (1979).
5. T. R. Osborn and W. R. Crawford, in *Air-Sea Interaction*, F. Dobson, L. Hasse, R. Davis, Eds. (Plenum, New York, 1980).
6. T. Curran, personal communication.
7. T. R. Osborn, *J. Phys. Oceanogr.* **10**, 83 (1980).
8. W. R. Crawford and T. R. Osborn, *Deep-Sea Res.* **26** (Suppl. 2), 309 (1979).
9. M. Tsuchiya, *Johns Hopkins Oceanogr. Stud.* No. 4 (1968).
10. *J. Mar. Res.* **37**, 399 (1979).

30 October 1980; revised 7 January 1981